Journal of Magnetic Resonance 212 (2011) 460–463

Contents lists available at SciVerse ScienceDirect

Journal of Magnetic Resonance

journal homepage: www.elsevier.com/locate/jmr

Communication

An NMR thermometer for cryogenic magic-angle spinning NMR: The spin-lattice relaxation of ^{127}I in cesium iodide

Riddhiman Sarkar [a], Maria Concistrè [a], Ole G. Johannessen [a,b], Peter Beckett [a], Mark Denning [a], Marina Carravetta [a,*], Maitham al-Mosawi [b], Carlo Beduz [b], Yifeng Yang [b], Malcolm H. Levitt [a,*]

[a] School of Chemistry, University of Southampton, SO17 1BJ, United Kingdom
[b] School of Engineering Sciences, University of Southampton, SO17 1BJ, United Kingdom

ARTICLE INFO

Article history:
Received 11 July 2011
Revised 8 August 2011
Available online 17 August 2011

Keywords:
Solid state NMR
Magic angle spinning (MAS)
Temperature measurement

ABSTRACT

The accurate temperature measurement of solid samples under magic-angle spinning (MAS) is difficult in the cryogenic regime. It has been demonstrated by Thurber et al. (J. Magn. Reson., 196 (2009) 84-87) [10] that the temperature dependent spin-lattice relaxation time constant of ^{79}Br in KBr powder can be useful for measuring sample temperature under MAS over a wide temperature range (20–296 K). However the value of T_1 exceeds 3 min at temperatures below 20 K, which is inconveniently long. In this communication, we show that the spin-lattice relaxation time constant of ^{127}I in CsI powder can be used to accurately measure sample temperature under MAS within a reasonable experimental time down to 10 K.

1. Introduction

The estimation of the real sample temperature in solid state NMR under magic angle spinning (MAS) is difficult for the following reasons: (i) it is difficult to place an independent temperature sensor directly inside the spinning rotor; (ii) frictional heating can modify the sample temperature; and (iii) the sample is exposed to several gas flows which may all be at different temperatures. Knowledge of the real sample temperature is essential for the study of molecular motion, as well as the electronic properties of organic conductors, superconductors and other interesting materials. Although optical temperature sensors function at low temperatures [1] and may be placed very close to the spinning rotor without an appreciable effect on the field homogeneity, there is no known method for placing them in contact with the spinning sample. NMR methods for determining the internal temperature of the sample itself are therefore preferable. Chemical shift changes at known phase transitions may be used as fixed calibration points [2–4]. Temperature-dependent changes in electric quadrupolar couplings [5,6], chemical shifts [7–13], dipolar couplings [14], and spin-lattice relaxation times [10] have all been used to provide NMR thermometers active over certain temperature ranges. For example the chemical shift of ^{207}Pb in $Pb(NO_3)_2$ can be used as a thermometer for a temperature range of 100–423 K [7–9], whereas the chemical shift of ^{79}Br in KBr is linearly dependent on temperature down to 100 K [10]. The chemical shift of ^{15}N in organic dye TTAA can be used as a thermometer over a temperature range of 130–405 K [11], whereas the chemical shift of ^{119}Sn in $Sm_2Sn_2O_7$ has been used for temperature measurements down to 85 K [12,13]. However at lower temperatures the chemical shifts of these substances become temperature independent. The proton lineshapes of some endohedral dihydrogen–fullerene complexes are temperature dependent below 50 K and may be used for temperature calibration [14].

It is our interest to perform solid state NMR below 20 K under magic angle spinning. Recently Thurber et al. [10] showed that the spin-lattice relaxation time constant (T_1) of ^{79}Br in KBr powder may be used to estimate the sample temperature under MAS, even at low temperatures down to 20 K. The dependence of T_1 on the temperature T was fitted to an empirical expression:

$$T_1 = \sum_{n=0,2,4,6} c_n T^{-n} \quad (1)$$

where in principle, the coefficients c_n are field-dependent. The coefficients for ^{79}Br in KBr at a field of 9.4 T, as reported by Thurber et al. [10], are given in the first row of Table 1.

The T^{-6} dependence leads to impractically long relaxation times (exceeding 3 min) at temperatures below 20 K. It is therefore necessary to find an alternative method for measuring the sample temperature at temperatures below 20 K.

* Corresponding authors. Fax: +44 23 8059 378.
E-mail addresses: M.Carravetta@soton.ac.uk (M. Carravetta), mhl@soton.ac.uk (M.H. Levitt).

1090-7807/$ - see front matter © 2011 Elsevier Inc. All rights reserved.
doi:10.1016/j.jmr.2011.08.021

Table 1
Coefficients from Eq. (1) found by fitting the experimental T_1 data.

Powder	Nucleus	Field (T)	Larmor frequency (MHz)	$c_0 \times 10^3$ (s)	$c_2 \times 10^{-3}$ (s K^2)	$c_4 \times 10^{-6}$ (s K^4)	$c_6 \times 10^{-9}$ (s K^6)
[a]KBr	^{79}Br	9.4	80.025	14.5	5.33	14.2	2.48
KBr	^{79}Br	14.1	150.313	8.7 ± 0.8	6.01 ± 0.03	12.2 ± 0.1	5.12 ± 0.05
RbBr	^{79}Br	14.1	150.313	5.9 ± 0.6	4.74 ± 0.02	5.9 ± 0.1	2.08 ± 0.08
CsBr	^{79}Br	14.1	150.313	5.5 ± 0.2	6.47 ± 0.01	3.94 ± 0.03	0.52 ± 0.01
CsI	^{127}I	14.1	120.041	−1.6 ± 0.5	1.52 ± 0.01	0.387 ± 0.03	0.121 ± 0.001

[a] Fitted coefficients for KBr from Thurber et al. [10] measured at 9.4 T.

2. Relaxation of halide nuclei in alkali halides

2.1. Relaxation mechanism

The relaxation mechanism for the spin-lattice relaxation of the halide nuclei in alkali metal halides is mainly quadrupolar above 10 K [15] and has been studied by van Kranendonk [16]. The quadrupolar spin-lattice relaxation takes place by a Raman process involving two acoustic phonons, where the energy from a spin transition is absorbed by the lattice leading to creation of one phonon and destruction of another. The energy difference between the two phonons is given by the Zeeman energy. As described in references [15–17], the spin-lattice relaxation rate depends on several parameters such as the mass density of the crystal, lattice parameters, velocity of sound, the quadrupole matrix element, the coupling of the lattice phonons with the nuclear quadrupole moment and the Debye temperature of the crystal. The mass density and lattice spacing for the alkali halides increase with the mass of the alkali metal, while the Debye temperature and velocity of sound in the crystal decrease. Thus, it is difficult to predict a trend of T_1 depending on these parameters. Nevertheless, we have observed experimentally that alkali halides with higher mass densities have faster spin-lattice relaxation for the halide nuclei at low temperatures (Figs. 1 and 2).

The quadrupolar splittings observed in the halide NMR spectra of the cubic alkali metal halides are usually attributed to crystal strain. However, such strain does not play a significant part in the relaxation of the nuclei at temperatures $\geqslant$10 K. T_1 shows no appreciable difference between different samples of the same compound [15].

2.2. Alkali metal bromides

The T_1 of ^{79}Br was measured as a function of temperature for the series of alkali metal bromides KBr, RbBr and CsBr using a static cryogenic NMR probe (see Experimental section). The temperature-dependence of the relaxation time constant was fitted to Eq. (1). The estimated coefficients c_n and their confidence intervals are reported in Table 1. The confidence intervals were derived from the uncertainty in the T_1 values, obtained by non-linear fits of the experimental saturation-recovery curves. The uncertainty in the estimated temperature (always below ±0.15 K) was neglected.

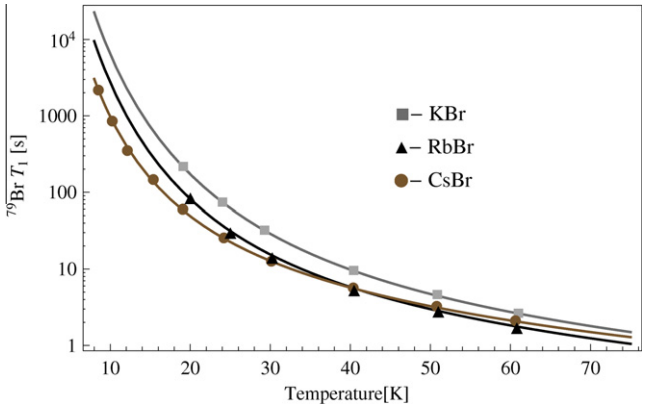

Fig. 1. T_1 of ^{79}Br in KBr, RbBr and CsBr as a function of temperature at a field of 14.1 T. The solid lines are fits to Eq. (1) with the coefficients shown in Table 1.

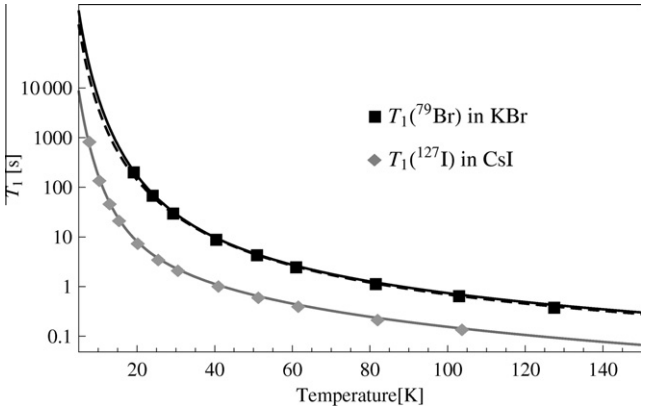

Fig. 2. Symbols: ^{79}Br and ^{127}I T_1 values in KBr and CsI respectively at a field of 14.1 T. Solid lines: fits of the T_1 values to Eq. (1), using the coefficients in Table 1. Dashed line: ^{79}Br T_1 of KBr at a field of 9.4 T, from Thurber et al. [10].

We obtained a similar temperature dependence for the T_1 of ^{79}Br in KBr as Thurber et al. [10]. However we obtained slightly longer T_1 values than Thurber et al. [10] over the entire temperature range, with the discrepancy increasing at low temperature (Fig. 2). This discrepancy is probably due to the higher magnetic field used in our experiments.

Increasing the mass of the metal cation decreases the ^{79}Br T_1 value over a wide temperature range. However, the ^{79}Br T_1 still exceeds 3 min for temperatures below 15 K, even in the extreme case of CsBr.

2.3. ^{127}I NMR of cesium iodide

Faster spin-lattice relaxation at low temperatures is obtained by increasing the mass density further and by observing ^{127}I, which has a higher quadrupole moment than ^{79}Br. The measured temperature dependence of T_1 of ^{127}I in CsI is shown in Fig. 2. The coefficients c_n are reported in the last row of Table 1. The T_1 of ^{127}I is much more suitable for temperature estimations of very low temperatures. For example, the T_1 of ^{127}I in CsI is less than 10 s at 20 K, and is only 145 s at 10.2 K.

3. Cryogenic magic angle spinning NMR

Fig. 3 shows a magic-angle spinning ^{127}I NMR spectrum for CsI recorded at 16.0 ± 0.15 K at 14.15 kHz spinning frequency. We observed a linewidth of 1.1 kHz for ^{127}I in CsI for the central transition. The other peaks in the spectrum are spinning sidebands of the satellite transitions. As in the case of KBr, a small first-order

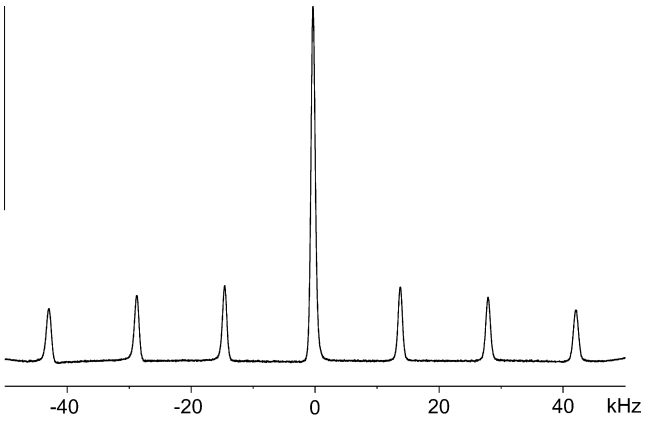

Fig. 3. Cryogenic magic-angle spinning ^{127}I NMR spectrum (two transients) of CsI recorded at a field of 14.1 T, a spinning frequency of 14.15 kHz, and a temperature of 16.0 ± 0.15 K.

quadrupolar interaction is observed (presumably due to strain in the cubic crystal). The first-order quadrupolar interaction forms rotational echoes under magic-angle spinning, giving rise to the prominent satellite spinning sidebands in Fig. 3.

T_1 measurements on ^{127}I in CsI allow temperature calibration under MAS in a reasonable experimental time at temperatures down to about 10 K. Fig. 4 shows a correlation between the temperature of the sample exhaust gas and the estimate of the sample temperature derived from ^{127}I T_1 measurements. The solid line is a linear fit to the equation $T_{sample} = 1.06 \times T_{exhaust} - 5.7$ K. The fit indicates that at a spinning frequency around 8 kHz, the temperature of the exhaust is 5.7 ± 0.8 K more than the true sample temperature. The discrepancy between the exhaust gas temperature and the sample temperature may be explained by the mixing of the cooling gas with the warm drive and bearing gases before leaving the spinning module. Studies of the relation between exhaust gas temperature and sample temperature as a function of spinning speed are under way.

4. Experimental

4.1. Thermometer calibration

A set of Cernox temperature sensors (part number CX-1070-SD, Lake Shore Cryotronics, Ohio, USA) were calibrated against a certified Rhodium–Iron resistance thermomemeter with a 4 mK accuracy (part number RF-100T-AA-1.4L, Lake Shore Cryotronics, Ohio, USA), by mounting all thermometers in a common oxygen-free high-conductivity copper block using high-thermal-conductivity grease and recording the resistance values sequentially as the temperature was slowly increased, starting at 4.2 K. The accuracy of the Cernox temperature calibration was better than ±0.15 K.

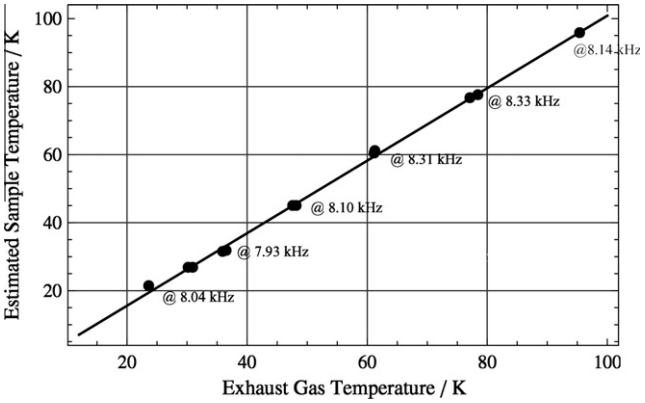

Fig. 4. Sample temperature estimated from the ^{127}I T_1 of CsI plotted against the temperature of the exhaust gas, in cryogenic magic-angle-spinning experiments. The spinning frequencies are indicated on the plot.

The Cernox sensor data sheets indicate a weak magnetic field dependence, with a systematic error of less than 1% in the estimated temperature at a field of 14.1 T. This was checked by comparing readings at a temperature of 4.2 K in zero and in 14.1 T magnetic fields. The magnetic-field dependence of the temperature readings is too small to be of concern in the current experiments.

4.2. Static experiments

The T_1 data in Figs. 1 and 2 were measured using a laboratory-built NMR probe placed in an Oxford Instruments continuous-flow cryostat (spectrostatNMR). This probe was designed to work at cryogenic temperatures, using helium gas to cool the non-rotating sample. One of the calibrated Cernox sensors was attached via an oxygen-free high-conductivity copper bridge to the 4 mm sapphire sample container to ensure good thermal contact with the NMR sample and minimization of temperature gradients. The copper bridge was insulated with cotton and teflon to provide thermal isolation from the cold helium gas stream, ensuring good thermal equilibrium with the sample. The probe contained several other Cernox temperature sensors at various points, but only the one in direct thermal contact with the sample was used as a reliable indicator of the sample temperature.

The NMR experiments were done at a field of 14.1 T. The T_1 estimations were made by saturation recovery experiments of the central NMR transition of ^{79}Br and ^{127}I. Optimum saturation was achieved with 250 $(\pi/2)$ pulses spaced by 150 μs. The nutation frequency was calibrated separately at each temperature, to take into account changes in electronic characteristics as the temperature is changed. 16 time-points, separated by a delay of 200 ms, were acquired for each saturation-recovery curve, with two transients averaged for each point. All saturation-recovery curves were found to fit well to a single-exponential recovery curve. The estimate of T_1 and the confidence intervals were obtained using the Levenberg–Marquardt method.

4.3. Cryogenic MAS

Our equipment for cryogenic magic-angle spinning NMR will be described in detail elsewhere. It differs from previous designs [6,14,18–20] by using three separate helium gas streams, one for the bearing system, one for the turbine system and one for sample cooling. All three cryogenic gas flows are generated from supercritical helium, created by warming liquid helium under a pressure of 3.0–4.5 bar in a large custom-built cryogenic boiler. The flow rates and temperatures of all three streams are independently controlled by using cryogenic needle valves and electrical heaters. The temperatures of the three gas streams are measured on entry to the probe cryostat.

The cryogenic spinning system uses a zirconia rotor with an outer diameter of 2 mm and length of 16.2 mm (including the turbine wheel inserts), provided by Revolution NMR (Fort Collins, CO). The temperature of the gas exiting the spinning assembly was monitored by using a Cernox temperature sensor mounted in the exhaust pipe about 2 cm from the rotor.

The T_1 measurements were made by following the intensity of the central transition peak in a saturation recovery procedure. The saturation of the central and all satellite transitions was ensured by applying a sequence of 250 $(\pi/2)$ pulses spaced by 150 μs.

5. Conclusions

The measurement of the ^{127}I spin-relaxation time constant in CsI allows estimation of the sample temperature in the cryogenic temperature range down to 10 K. The method is rapid, convenient, and is compatible with magic-angle spinning. The major disadvantage of using CsI instead of KBr is that the ^{127}I resonance frequency is far from that of common observable nuclei such as ^{13}C, while the resonance frequency of ^{79}Br and ^{13}C are conveniently close. The observation of the T_1 of ^{79}Br in CsBr is a reasonable compromise, allowing temperature calibration down to 15 K.

Acknowledgment

This research was supported by the Basic Technology Program (RCUK). RS acknowledges a Swiss National Science Foundation prospective researcher grant (PBELP2-130906).

References

[1] http://www.lakeshore.com/pdf_files/IRFILTERS/FOSdatasheet.pdf.
[2] J.F. Haw, R.A. Crook, R.C. Crosby, Solid–solid phase transitions for temperature calibration in magic-angle spinning, J. Magn. Reson. 66 (1986) 551–554.
[3] K.L. Anderson-Altmann, D.M. Grant, A solid-state 15N NMR study of the phase transitions in ammonium nitrate, J. Phys. Chem. 97 (1993) 11096–11102.
[4] H.H. Limbach, J. Hennig, R. Kendrick, C.S. Yannoni, Proton-transfer kinetics in solids: tautomerism in free base porphines by 15N CPMAS NMR, J. Am. Chem. Soc. 106 (1984) 4059–4060.
[5] R. Tycko, Adiabatic rotational splittings and berrys phase in nuclear-quadrupole resonance, Phys. Rev. Lett. 58 (1987) 2281–2284.
[6] R. Tycko, K.R. Thurber, Biomolecular solid state NMR with magic-angle spinning at 25 K, J. Magn. Reson. 195 (2008) 179–186.
[7] A. Bielecki, D.P. Burum, Temperature dependence of ^{207}Pb MAS spectra of solid lead nitrate. An accurate, sensitive thermometer for variable-temperature MAS, J. Magn. Reson., Ser A 116 (1995) 215–220.
[8] M. Concistrè, A. Gansmüller, N. McLean, O.G. Johannessen, I.M. Montesinos, P.H.M. Bovee-Geurts, P. Verdegem, J. Lugtenburg, R.C.D. Brown, W.J. DeGrip, M.H. Levitt, Double-quantum ^{13}C nuclear magnetic resonance of bathorhodopsin, the first photointermediate in mammalian vision, J. Am. Chem. Soc. 130 (2008) 10490.
[9] G. Neue, C. Dybowski, Determining temperature in a magic-angle spinning probe using the temperature dependence of the isotropic chemical shift of lead nitrate, Solid State Nucl. Magn. Reson. 7 (1997) 333–336.
[10] K.R. Thurber, R. Tycko, Measurement of sample temperatures under magic-angle spinning from the chemical shift and spin-lattice relaxation rate of ^{79}Br in KBr powder, J. Magn. Reson. 196 (2009) 84–87.
[11] B. Wehrle, F. Aguilar-Parrilla, H.H. Limbach, A novel 15N chemical-shift NMR thermometer for magic angle spinning experiments, J. Magn. Reson. 87 (1990) 584–591.
[12] C.P. Grey, A.K. Cheetham, C.M. Dobson, Temperature-dependent solid-state ^{119}Sn MAS NMR of $Nd_2Sn_2O_7$, $Sm_2Sn_2O_7$, and $Y_{1.8}Sm_{0.2}Sn_2O_7$. Three sensitive chemical-shift thermometers, J. Magn. Reson., Ser A 101 (1993) 299–306.
[13] T.F. Kemp, G. Balakrishnan, K.J. Pike, M.E. Smith, R. Dupree, Thermometers for low temperature magic angle spinning NMR, J. Magn. Reson. 204 (2010) 169–172.
[14] M. Carravetta, O.G. Johannessen, M.H. Levitt, I. Heinmaa, R. Stern, A. Samoson, A.J. Horsewill, Y. Murata, K. Komatsu, Cryogenic NMR spectroscopy of endohedral hydrogen-fullerene complexes, J. Chem. Phys. 124 (2006).
[15] C.E. Tarr, L.M. Stacey, C.V. Briscoe, Nuclear spin-lattice relaxation in alkali halides at low temperatures, Phys. Rev. 155 (1967) 272–278.
[16] J.v. Kranendonk, Theory of quadrupolar nuclear spin-lattice relaxation, Physica 20 (1954) 781–800.
[17] E.G. Wikner, W.E. Blumberg, E.L. Hahn, Nuclear quadrupole spin-lattice relaxation in alkali halides, Phys. Rev. 118 (1960) 631–639.
[18] A. Hackmann, H. Seidel, R.D. Kendrick, P.C. Myhre, C.S. Yannoni, Magic-angle spinning NMR at near liquid–helium temperatures, J. Magn. Reson. 79 (1988) 148–153.
[19] P.C. Myhre, G.G. Webb, C.S. Yannoni, Magic angle spinning nuclear magnetic resonance near liquid–helium temperatures. Variable temperature CPMAS spectra of the 2-norbornyl cation to 6 K, J. Am. Chem. Soc. 112 (1990) 8991–8992.
[20] P.C. Myhre, G.G. Webb, C.S. Yannoni, Magic angle spinning nuclear magnetic resonance near liquid–helium temperatures. Variable-temperature CPMAS studies of C_4H_7+ to 5 K, J. Am. Chem. Soc. 112 (1990) 8992–8994.